

CATALYST AND PROCESS DEVELOPMENT FOR SYNTHESIS GAS CONVERSION TO ISOBUTYLENE

by

Rayford G. Anthony and Aydin Akgerman

Project Team and Contributors to This Report
Dr. C. V. Philip, Associate Research Scientist
Dr. Can Erkey, Post Doctoral Research Associate
Z. (Jeffrey) Feng, Ph. D. Student
Walter Postula, Ph. D. Student

DOE Contract No. DE-AC22-90PC90045
Texas A&M Research Foundation Project No. 6722

OBJECTIVES

The objectives of the project are: (1) To synthesize new catalysts; (2) To develop kinetic and reactor models for fixed bed trickle flow, slurry flow, and fixed bed gas phase reactors; and (3) to simulate and optimized the performance of these reactors for conversion of hydrogen lean synthesis gas to isobutylene. To accomplish the stated objectives of the project, five major tasks have been defined. The first two are short term and consist of performing a thorough review of the literature, including the patent literature to identify the proven catalysts for isobutylene synthesis, and to begin the modification of existing bench scale equipment to perform the evaluation of catalysts and development of kinetic data. A preliminary literature search was conducted in the preparation of the proposal, however, this area was revisited to insure that no important work reported in the literature was overlooked. The other three tasks are on synthesis, characterization and activity testing of potential catalysts, development of kinetic models for the respective catalysts, and optimization of the reactor configuration to maximize production of isobutylene. This report highlights the accomplishments with primary emphases on establishing base line results.

BACKGROUND

Earlier work on isobutylene and isobutane synthesis employed thorium based catalysts. Later isoalkenes were produced when zirconia was used at lower pressures and temperatures of 623 to 673 K. These difficultly reducible oxide catalysts such as ThO_2 (Pichler and Ziesecke,

1950a&b) and Dy_2O_3 , (Kieffer et al. 1983) were used under very severe conditions. A CdO catalysts combined with acid supports was used under mild conditions. Recently (Maruya, et al., 1988 and Onishi et al., 1988) have reported the use of ZrO_2 at mild conditions, and methoxide species and formate ions have been observed on the surface of the ZrO_2 catalysts. The mechanisms for formation of the branched alkanes has been postulated to be different than the mechanism for formation of linear alkanes.

It is believed (Vedage et al. 1985) that linear products are produced by CO insertion into an alkoxide instead of an aldol-like condensation scheme in which a formyl species reacts with an enolate ($\text{RCH}_2\text{-HCHO}$) at the carbon next to the carbonyl carbon. Mazanec (1986) proposed a CO insertion scheme involving a bound aldehyde to produce a cyclic acyl which has a two valence structures and the carbonyl carbon in one has carbenic character. Subsequent 1,2 shifts of hydrogen or R can lead to linear or branched products. Condensations reactions between eta-enolates and alkoxides were proposed to account for deviations from the Schulz-Flory distribution. Tseng et al. (1988) and Jackson and Ekerdt (1990) present the results of a comprehensive study and detailed discussion of proposed mechanisms on isosynthesis using zirconia. The formation of C_4s is postulated to be by addition and condensation reactions (Maruya, et al. 1988, 1989; Tseng et al., 1988; Jackson and Ekerdt, 1990).

Pichler and Ziesecke (1950a&b) performed much of the pioneering work on conversion of synthesis gas to isoalkanes with high yields to isobutane and isobutylene. Severe conditions (300 atm. and 673 K) were used for this synthesis. Zirconia was found by Pichler and Ziesecke to be the second most active catalysts for the isosynthesis reaction. Maruya, et al. (1989) producing a C_4 fraction with 99+ % isobutylene, but the carbon C_4 selectivities were in the range of 77 to 85% . The latter value was obtained when zirconia was impregnated with NaOH.

CATALYSTS SYNTHESIS AND CHARACTERIZATION

Synthesis: Three types of synthesis procedures are to be used in the project. They are the precipitation from inorganic salts, such as zirconyl chloride or zirconyl nitrate with ammonium hydroxide or a hydroxide from group 1 of the periodic table. These materials will be referred to as preparation method 1, i.e. Cat. #1. For example data presented herein will be on catalysts prepared by precipitation of zirconyl nitrate with ammonium hydroxide. The catalysts are labeled CAT 1, batch 1,2,3 or 4. Catalysts prepared by the Sandia procedure (Dosch et al.,

1990a & b and Stephens et al., 1985) developed by Dosch for hydrous metal oxides will be referred to a CAT. 2. Data are presented herein for Cat. 2. Method 3 consists of using the method developed by Anthony and Dosch (1990) for the preparation of a new series of titanates. Zirconium will be used instead of titanium in the preparation. No data will be reported in this paper on Cat. No. 3.

Characterization: Differentiation between cubic zirconia and tetragonal zirconia by use of XRD has been reported to be very difficult and impossible. Cubic zirconia is normally formed at temperatures above 1200 °C except in the presence of alkali or alkaline salts. The cubic form can then be stabilized at lower temperatures. Inspection of XRD powder patterns suggests that one should be able to distinguish between the cubic and tetragonal forms. However, this is very difficult to accomplish except for highly crystalline zirconia. Figures 1 through 3 illustrate XRD spectra of Cat. #1 Batch #1. Shortly after calcination, the zirconia appeared to be cubic, but was most probably composed of tetragonal and very small crystallites of monoclinic zirconia. Figures 2 and 3 illustrate XRD diffraction pattern and a Raman spectra after 6 months, and the Raman spectra clearly shows the presence of the monoclinic and tetragonal phases. The monoclinic phase based on Raman spectroscopy appears to be the dominate phase. The XRD pattern might lead one to believe otherwise. Using the same procedure as in Batch #1, Cat. No. 1, three additional batches were prepared and they all were monoclinic based on the XRD pattern. Activity data reported herein for Cat. 1 is for batches 3 and 4, because they were initially only monoclinic.

Figure 4 illustrates the titration curve for hydrous sodium zirconium oxide prepared by Dosch's method. the sodium content was decreased to a small level using HCl exchange, and then calcined at 500 °C for 4 hours. The zirconia formed by this method should be more acidic than the zirconia prepared according to procedure #1. The sodium can be removed by ion exchanging with ammonium hydroxide/chloride solution at a high pH and then calcined. Zirconia synthesized with this method will be more basic than when using HCl to remove the sodium. However, the catalyst #2 activity reported herein is for the HCl exchanged catalysts. After calcination Catalyst #2 appeared to be monoclinic. Jackson and Ekerdt (1990) have reported that the catalytic activity does not appear to be a function of the particular phase.

BENCH SCALE UNITS AND PROCEDURES USED IN EVALUATING THE CATALYSTS ACTIVITIES

Bench-Scale Unit #1: A schematic diagram of BSU1 is shown in Figure 5. The feeds CO and H₂ are metered with mass flow meter-controllers, pass through a mixer, into a preheater contained in the oven I, and into a 3/8" reactor. The effluent from the reactor is passed through a back-pressure regulator, a liquid gas separator (L), and to a three-way valve which can be turned to vent the product gases into a hood, or pass the product gases through a gc sample loop to a bubble meter and then vent into a hood. A nitrogen purge line is also connected to the reactor. Molecular sieve (5A) dryers are on each of the feed lines for removal of residual moisture from the feed gases, and a charcoal filter is on the CO line to remove carbonyls. For this report the gc column is picric acid on Carbopak. Propylene, the C₄s and higher molecular weight hydrocarbons are separated on this column. The gc is equipped with FID and TCD detectors. A gas sampling port is also located at M for collecting samples for off-line analysis on a Carle gc equipped with several columns and switching valves. Hydrogen, carbon monoxide, carbon dioxide, methane, ethane, ethylene, propane, propylene, each of the butylenes, butadiene, isobutane and n-butane and C₅⁺ hydrocarbons are obtained. The oxygenates, methanol, dimethyl ether, and water, are determined off-line by using a Gow-Mac gc equipped with a Poropak Q column. In the reactor thermocouples are located at the beginning and end of the bed. Some product is condensed in the trap L. These were high boiling hydrocarbons with which eluted on a gc with a macrobore silica column over the temperature range of 160 to 200 °C. Twenty four to forty eight hours of operation were required to detect the formation of these high molecular weight products. They are estimated to account for less than 1 %(w) of the hydrocarbon product produced.

Bench-Scale Unit No. 2: Bench unit No. 2 used in this work is a CDS 900 totally automated reactor-gc system. A schematic diagram is presented in Figure 6. (This unit is currently manufactured by Autoclave Engineers and called an AE MSBTR 900.) Nitrogen purge lines are not shown on this diagram. All of the lines from the reactor are heated to 180 °C, and no condensate is collected prior to analysis using the on-line gc. The on-line gc uses a palladium transfer tube for hydrogen analysis, a mole sieve for methane and CO; a Poropak Q for analysis of CO₂, methanol, water, dimethyl ether, ethane, ethylene, propane, propylene, isobutane, butane,

total butylenes, and other oxygenates using a TCD detector; and a macrobore silicon column with 5% methyl phenyl coating and a FID detector for determining the composition of the hydrocarbons produced. Isobutylene composition is determined by off-line analysis using the Carle gc described above. Since the analysis with the Carle yields some of the same information as the on-line analysis, the results are compared to determine if sample is lost in the process of sampling and analyzing off-line. The C_3^+ fraction from the Carle is usually 1 to 5% less than the C_3^+ fraction from the on line analysis.

A schematic of the reactor and ovens are shown in Figure 7. The reactor oven is maintained at a temperature of 180 °C, and the separate furnaces on the reactor tube are used to control reaction temperature. Liquid CO_2 can be fed to the heat exchanger located on the reactor tube to quench the reaction products. However, no CO_2 quenching was done in this study. A thermowell is located down the center of the 1/2" i.d. reactor tube, and used to measure the temperature profile with nitrogen flowing through the system and during the reaction. Figures 8 and 9 illustrate measured temperature profiles with and without reaction, and Figure 9 illustrated the simulation of the temperature profile from a reactor model for the unit. The catalyst is located in the isothermal portion of the reactor, i.e. between 20 to 25 cm. All three reactor heaters were maintained at the same temperature for this study, but a larger isothermal region should be the result by increasing the reactor heater temperatures at the top and bottom of the reactor.

For both systems the catalysts was loaded and purged with nitrogen at 400 °C for 4 hours prior to conducting the activity studies. Catalytic activity data reported herein for the precipitated catalysts, Cat. #1 batches 3 and 4, were obtained in the BTU1, and catalytic activity data reported for Cat. #2 were obtained using the AE MSBTR 900.

CATALYSTS EVALUATION

Figure 10 illustrates the activity and effect of pressure on CO conversion for zirconia using preparations 1&2. Preparation #2 is designated by the (\$ Feng @ 425). The space time, τ , is defined as the bulk volume of the catalysts divided by the volumetric feed rate calculated at reaction conditions. The actual residence time is greater than the space time because of the decrease in the number of moles with reaction. However, at low conversions space time is a close approximation to residence time, which is dependent on the extent of reaction. Figure 10

illustrates that pressure does not have a significant effect on conversion at equal space times for a 1:3 or a 1:1 CO:H₂ ratio. Similarly results were obtained by Pichler and Ziesecke (1950 a&b) for thoria catalysts. The data also seems to suggest that Cat. #2 is not as active as Cat. #1. Figures 11 and 12 illustrate the expected trend for change in conversion with space time at 95 atm. and 400 °C. Space times of 90 seconds are required to obtain 20% CO conversion. Figure 13 illustrates the expected increase in conversion with increasing temperature for the two catalysts. The trends are the same indicating essentially the same reaction mechanism and activation energy.

Figure 14 illustrates the long term activity of catalyst #2. There appears to be an increase in activity with time on stream. All of the previous data were reported after approximately two hours on stream. However, based on the results from Figure 14 longer times at a fixed set of conditions may be required to reach a true steady state in relation to CO conversion. The amount of isobutylene in the C₄ fraction did not change with time on stream. Reaction stoichiometry appears to correspond primarily to that for the formation of olefins, alkanes and carbon dioxide.

The usage ratio of hydrogen to carbon monoxide was 0.53 ± 0.01 , and with the exception of methane formation the hydrocarbon distribution appears to be predominately olefins.

In order to gain some insight into the type of reactions occurring several ratios were calculated, and are presented Table 1. Table 1 illustrates the average values obtained for the isosynthesis profile, the branched to linear C₄s and the isobutylene selectivity within the C₄ fraction. The isosynthesis profile was defined by Jackson and Ekerdt as the ratio of C₄s to (ethane + propane). Jackson and Ekerdt used a molar ratio, but the data presented in Table 1 are weight ratios. Data reported by Jackson and Ekerdt and data obtained for Catalysts #1 and #2, respectively are presented. The isosynthesis profile is a measure of the relative importance of the condensation reactions. The data shown in Table 1 did not appear to show any trends because of the large error bands on the experimental points. Further work on refining the analytical and sampling procedures is required to determine if a trend exists with a variation in temperature, pressure, space time and CO:H₂ ratio. Ratios and the profile obtained in this study are comparable with the values reported by Jackson and Ekerdt (1990).

Figures 16, 17 and 18 illustrate the effect of pressure, space time, and CO:H₂ ratio on the molar ratio of isobutylene to methane and the weight ratio of isobutylene to C₅⁺ for Cat. #1. For

a 1:3 CO:H₂ ratio the isobutylene to C₅⁺ decreases as the pressure is increased, but the molar ratio of isobutylene to methane is essentially constant at 0.3. These conditions correspond to CO conversions less than 5%. However, at 95 atm and a 2:1 CO:H₂ ratio, the isobutylene to methane molar ratio varies from 0.5 to 0.75 as the CO conversion is increased with an increase in residence time.

Figure 19 shows a comparison of catalysts preparation procedures. An increase in the weight ratio of isobutylene to C₅⁺ catalysts show the same increasing trend with increasing temperature. Figure 20 shows a comparison of the weight ratio of isobutylene to methane for Catalysts #1 and #2. For Catalyst #2 a decrease in the ratio is observed with increasing temperature. For Catalysts #1, a trend with increasing temperature is not observed. Obviously more data are needed to fully substantiate these results, since only two points at comparable space time were measure for each catalyst.

MACRO AND MICRO KINETIC MODELS

Macrakinetic models: Two approaches are being used to develop kinetic models for isobutylene synthesis from hydrogen lean synthesis gas. The first is to examine surface response models over comparable ranges of conversion and the parameter $kRT\tau$. Maruya et al. (1988) report a second order dependence on carbon monoxide and a first order dependence for hydrogen at pressures of 69 kPa (0.69) atmospheres. We considered these results and the possibility of reaction orders of first order CO and first order hydrogen, and second order hydrogen and first order CO. Utilizing the data from our experiments, a range of values for $kRT\tau$ which would give reasonable conversions were determined. The equations for these three cases at low conversion, which corresponds to only a small change in volumetric flow rate due to the decreasing stoichiometry of the reaction, are presented as follows.

Second Order CO and First Order H₂:

$$k R T \tau = \frac{2}{P_A^0 P_B^0 (2-\beta)} \left[\frac{x}{1-x} - \frac{\beta}{2-\beta} \log_e \frac{1-0.5\beta x}{1-x} \right] \quad \beta=2 \quad (1)$$

$$k R T \tau = \frac{2 x x^2}{2 p_A^0 p_B^0 (1-x^2)} \quad \beta=2 \quad (2)$$

$\beta = p_A^0/p_B^0$, the ratio of the initial partial pressures of A and B, where A = CO and B = H₂.

The stoichiometry, which was used, is for the reaction to produce olefins and CO₂.

First Order CO and Second Order H₂:

$$k R T \tau = \frac{2}{(p_B^0)^2 (\beta-2)} \left[\frac{\beta/2 x}{1-\beta/2} - \frac{2}{\beta-2} \log_e \frac{1-x}{1-\beta/2 x} \right] \quad \beta \neq 2 \quad (3)$$

For $\beta = 2$

$$k R T \tau = \frac{2 x - x^2}{2 (p_A^0)^2 (1-x)^2} \quad (4)$$

First Order CO and First Order H₂:

$$k R T \tau = \frac{2}{p_B^0 (2-\beta)} \log_e \frac{1 - 0.5 \beta x}{1-x} \quad \beta \neq 2 \quad (5)$$

For $\beta = 2$

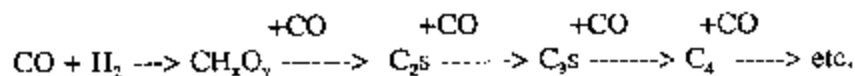
$$k R T \tau = \frac{x}{p_B^0 (1-x)} \quad \beta=2 \quad (6)$$

The left hand side of Equations (1) through (6) is a function of temperature and space time, and has the units of reciprocal atm. to the first or second power. The right hand side of these

equations is a function of conversion, pressure and the feed composition. The unit on the right hand side are also reciprocal atm.

Figures 20, 21, and 22 illustrate plots of these equation for the different orders and feed compositions. The most interesting feature of these graphs are the low conversion predicted for first order hydrogen and first order carbon monoxide. The second interesting feature is the shifting of the curves for CO:H₂ feeds of 1:3 and 2:1 for the two reaction orders shown. The conversions obtained in this study appear to be representative of Equations 1 through 4. Additional work is required to discriminate between these equations.

The approach represented above could be the first step in a series, parallel reaction sequence of the following type.



With the exception of the formation of CH_xO_y and the C₂S, condensation reactions would also occur in addition to CO insertion. This macro reaction sequence needs further refining to account for branching reactions.

Micro Kinetic Model: A micro kinetic sequence is being developed based on elementary steps. The mechanisms presented by Tseng et al. (1988), Maruya et al. (1988 and 1989) and Jackson and Ekerdt (1990) are being used in development of the microkinetic model. In addition, the bond energies of each elementary step are calculated using the Bond Order Conservation Theory of Schusterovich. This approach is the group contribution method which involves the use of heats of chemisorption of atoms of O, H, and C on metal surfaces to calculate the heats of chemisorption of molecular species. The heats of chemisorption of O and H on zirconia were estimated using literature data. The values for C were extrapolated based on the periodic table. These heats of chemisorption of individual atoms when combined with gas phase dissociation energies enables one to calculate the activation energies. A total of 68 equations have been postulated to occur. The theory has been developed for metals, and we are extending the method to the metal oxides.

The results of the initial calculations are encouraging because the activation energies which have been calculated suggest reaction pathways which have been proposed by others

(Jackson and Ekerdt, 1990). Table 2 list the reaction sequences and activation energies calculated to date. Many additional steps are required to complete the model for isobutylene synthesis.

REACTOR MODELS

Substantial progress has been made in developing a reactor model for the trickle bed reactor for isobutylene synthesis from synthesis gas. As a first approximation a molecular second order reaction is being used to develop the basic algorithm. Further work will be required when a kinetic rate equations have been developed. Figures 23 through 26 show the dimensionless equations and boundary conditions and some typical results obtained for the proposed model. Gas and liquid concentration profiles are calculated, and a profiles of the concentration of reactants and products within the pores are also illustrated. Resistance to diffusion of the reactants and products are illustrated in Figure 26. If no resistance to diffusion existed the concentrations would be uniform throughout the catalyst pellet.

SUMMARY OF ACCOMPLISHMENTS AND FUTURE PLANS

The bench scale reactor systems have been successfully operated for a period of approximately one month with substantial amount of data obtained. The data reported above are for Batches 3 and 4 of catalysts preparation Cat. #1. Data were also obtained on a catalyst prepared by catalyst preparation #2. Batches 2 and 3 for preparation of Cat. 1 were chosen because the XRD patterns and Raman spectra indicated they were predominately monoclinic, and unlike the result obtained for batch #1, the XRD pattern did not change after the first calcination. Cat. 2 was used to illustrate the performance of the AE MSBTR 900 for this system. Experiments are planned for the AE MSBTR 900 reactor system using preparation, Cat. #1, to produce the zirconia. The objective of these experiments is to verify that the same or nearly the same results are obtained when using either reactor system. The experimental procedures used to obtain the data presented herein needs to be refined. Our gc-ms is being repaired so the type (olefins, alkanes, oxygenates) of the higher molecular weight compounds can be determined.

Several methods of preparing the zirconia will be investigated to determine the effect of calcination and drying on the catalysts activity. Methods to be used are supercritical extraction, coating of pre-engineered supports. Removing the sodium or potassium from the hydrous zirconium oxide by ion exchanging with ammonium hydroxide or ammonium chloride, followed

by filtering, drying and calcination. We also plan to evaluate catalysts prepared by using Cat. prep. #3. It is well known that the method of preparation can greatly affect the catalytic activity. For example, the mixed oxides of MgO-TiO₂ (10% MgO) and TiO₂-SnO₂ when calcined in vacuum have high basicities, (Tanabe, 1970 and 1981). Recent work reported at the 12th North American Catalysts Society Meeting in Lexington, KN (May, 1991) showed the effect on zirconia surface area by using supercritical extraction to prepare the zirconia. We plan to make significant progress in the synthesis of isobutylene in the next year.

LITERATURE CITED

- Anthony, R. G. and Dosch, R. G., "Catalysts and Preparation of New Titanates," in *Preparation of Catalysts V*, Ed. Poncelet, G. P. A. Jacobs, P. Grange and B. Delmon, Elsevier Science Publishers B. V., Amsterdam, pages 637-646 (1990).
- Dosch, R.G., Stephens, H. P., and Stohl, F. V., SAND89-2400, Sandia National Laboratories, 1990a.
- Dosch, R. G., Stephens, H. P., and Stohl, F. V., SAND8902400, Sandia National Laboratories, 1990b.
- Holland, C. D. and R. G. Anthony, *Fundamentals of Chemical Reaction Engineering*, Prentice-Hall Inc., Engelhard, NJ (1989).
- Kieffer, R., G. Cherry, and R. E. Bacha, "Carbon Monoxide-Hydrogen Reactions. Mechanism of Isobutane Formation in Isosynthesis," *Mol. Chem.*, 2(1), 11-23 (1983).
- Jackson, N. B. and Ekerdt, J. G., "The Surface Characteristics Required for Isosynthesis over Zirconium Dioxide and Modified Zirconium Dioxide," *J. of Catal.* 126, 31-45 (1990).
- Mazanec, T. J., "On the Mechanism of Higher Alcohol Formation Over Metal Oxide Catalysts" *J. Catal.* 98, 115 (1986).
- Maruya, K., T. Maehashi, T. Haraoka, S. Narui, Y. Asakawa, K. Domen, and T. Onishi, "The CO-H₂ Reaction over ZrO₂ to Form Isobutene Selectively," *Bull. Chem. Soc. Jpn.*, 61, 667-671 (1988).
- Maruya, K., T. Fujisawa, A. Takasawa, K. Domen and T. Onishi, "Effect of Additives on Selective Formation of Isobutene from the CO-H₂ Reaction over ZrO₂," *Bull. Chem. Soc. Jpn.*, 62, 11-16 (1989).
- Onishi, T., Maruya, K-I, Domen, K., Abe, H., and Kondo, J., "The Mechanism of CO Hydrogenation Over Zirconium Oxide Studied by FT-IR," *Catalysis: Theory to Practice*,

Vol. 2 (M. J. Phillips and M. Teman, Editors), Proceedings of the 9th International Congress on Catalysis, Calgary, (1988).

Pichler, H., and Ziesecke, K-H., "Über die bei der Isosynthese entstehenden sauerstoffhaltigen Verbindungen, unter besonderer Berücksichtigung der Alkole," *Brennst. Chem.*, 31, 360 (1950a).

Pichler, H., and Ziesecke, K-H., "The Isosynthesis," *Bur. Mines Bull.*, 488 (1950b).

Stephens, H. P., Dosch, R. G., and Stohl, F. V., *Ind. & Engr. Che., Prod. Res & Dev.*, 24, 15 (1985).

Tanabe, K., *Solid Acids and Bases*, Academic Press, New York (1970).

Tanabe, K., "Solid Acid and Base Catalysts," vol 2, pp. 231-273 in *Catalysis-Science and Technology*, Ed. J. R. Anderson and M. Boudart, Pub. Springer-Verlag, Berlin (1981)

Tseng, S. C., N. Jackson, and J. G. Ekerdt, "Isosynthesis Reactions of Carbon Monoxide/Hydrogen Over Zirconium Dioxide," *J. Catal.* 109(2), 284-297 (1988),

Vedage, G. A., P. G. Himerfarb, G. W. Simmons, and K. Klier, in "Solid State Chemistry in Catalysis" Eds. R. K. Grasselli and J. F. Bradzil, ACS Symposium Series No. 279 (1985).

Table 1. Isosynthesis Characteristics of Different Catalysts

Item	Catalyst #1	Catalyst #2	J&E ¹
Isosynthesis Profile ²	4.55±1.28	2.29±0.79	2.30
Branched/ Linear C ₄	2.71±0.67	2.97±0.33	0.18
i-C ₄ H ₈ / All C ₄ 's	0.63±0.06	0.37±0.15	0.84

¹ N.B. Jackson and J.G. Ekerdt (1990). 425°C, 35 atm, 1:1 H₂/CO

² Defined as (total weight of C₄ hydrocarbons / total weight of C₂'s and C₃'s)

All the ratios are calculated on weight basis.

Table 2 Microkinetic Reaction Parameters

Reaction	E_A^f (kcal/mol)	E_A^r (kcal/mol)
(1) $H_2 + 2Zr \rightleftharpoons 2ZrH$	15	-7
(2) $ZrH + ZrO \rightleftharpoons ZrOH + Zr$	45	26
(3) $CO + Zr \rightleftharpoons ZrCO$	-32	
(4) $ZrCO + Zr \rightleftharpoons ZrC + ZrO$	25	-32
(5) $ZrC + ZrH \rightleftharpoons ZrCH + Zr$	39	5
(6) $ZrCH + ZrH \rightleftharpoons ZrCH_2 + Zr$	18	23
(7) $ZrCH_2 + ZrH \rightleftharpoons ZrCH_3 + Zr$	5	33
(8) $ZrCH_3 + ZrH \rightleftharpoons CH_4 + 2Zr$		
(9) $ZrCH_3 + ZrH \rightleftharpoons ZrCH_4 + Zr$	1	34
(10) $ZrCO + ZrH \rightleftharpoons ZrOCH + Zr$	13	19
(11) $ZrOCH + Zr \rightleftharpoons ZrCH + ZrO$	31	51
(12) $ZrOCH + ZrH \rightleftharpoons ZrOCH_2$	33	3
(13) $ZrOCH_2 + Zr \rightleftharpoons ZrCH_2 + ZrO$	4	-24
(14) $ZrOCH_2 + ZrH \rightleftharpoons ZrOCH_3 + Zr$	-4	23
(15) $ZrOCH_3 + ZrH \rightleftharpoons ZrCH_3OH + Zr$		
(16) $ZrCH_3OH + Zr \rightleftharpoons ZrCH_3 + ZrOH$		
(17) $ZrOCH_3 + ZrH \rightleftharpoons CH_3OH + 2Zr$		
(18) $ZrCH_3OH + Zr \rightleftharpoons ZrCH_3 + ZrOH$		
(19) $ZrCO + ZrOH \rightleftharpoons ZrOOCH + Zr$	17	18
(20) $ZrOOCH + Zr \rightleftharpoons ZrOCH + ZrO$	13	45
(21) $ZrOOCH + ZrH \rightleftharpoons ZrHCOOH + Zr$		
(22) $ZrOOCH + Zr \rightleftharpoons ZrO_2C + ZrH$	21	-13

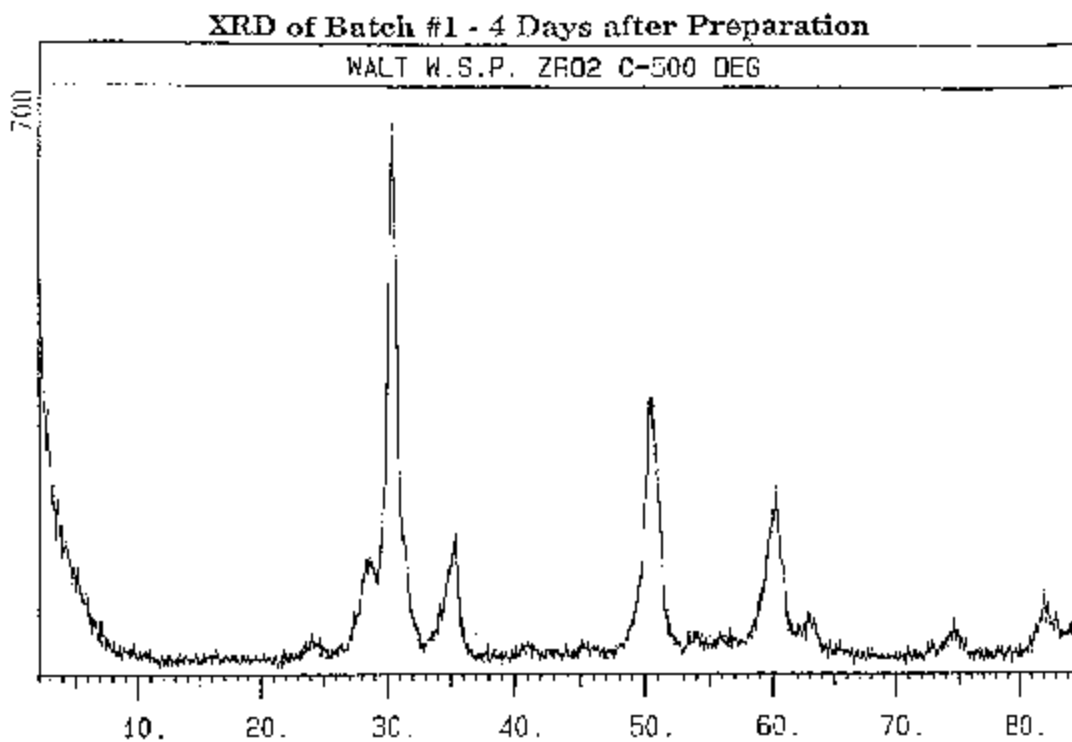


Figure 1. Catalyst #1, Batch #1 – XRD Pattern Indicates Formation of Cubic or Tetragonal Zirconia.

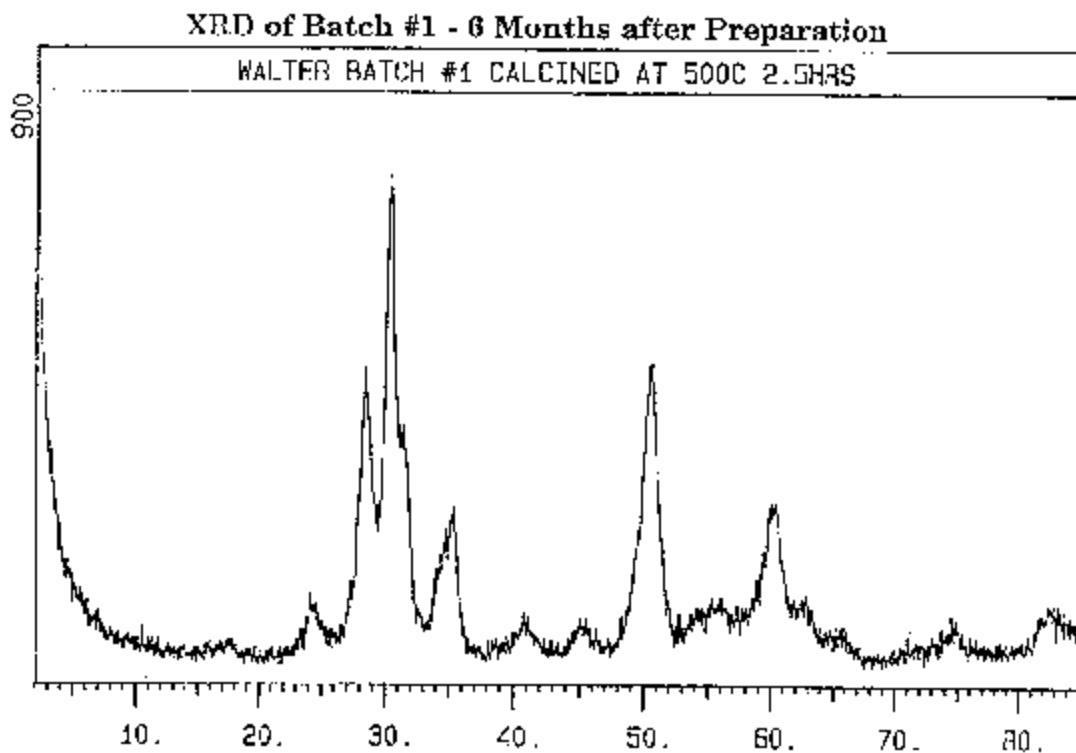


Figure 2. Catalyst #1, Batch #1 -- After Setting in Desiccator For Six Months.

Raman Spectra of Batch #1 - 6 Months after Preparation

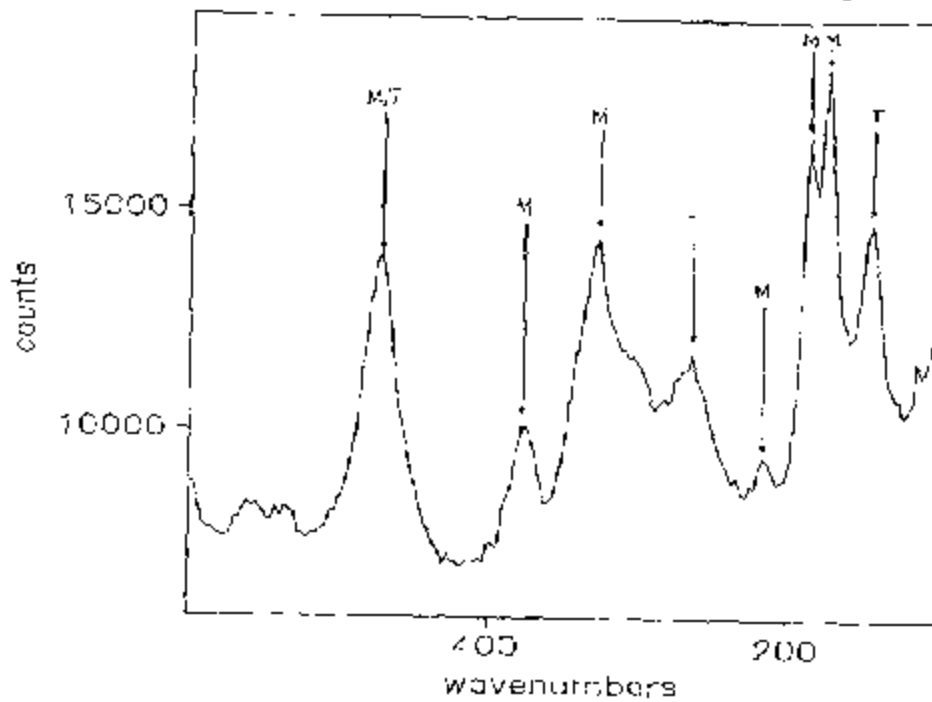


Figure 3. Catalyst #1, Batch #1 -- Raman Spectra Indicates Presence of Monoclinic and Tetragonal Zirconia.

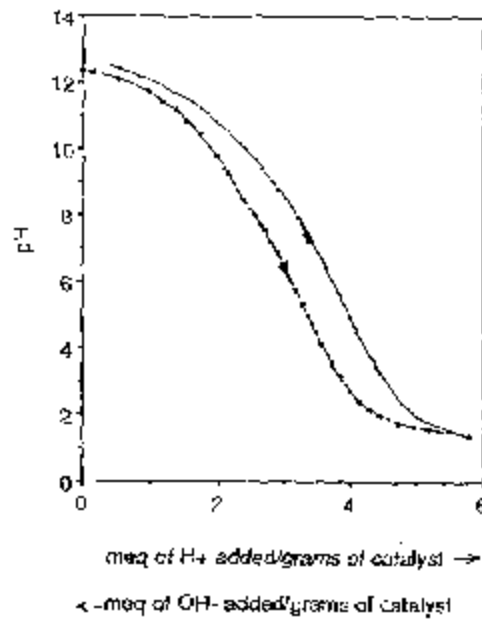


Figure 4. Titration Curve for Hydrous Sodium Zirconium Oxide.

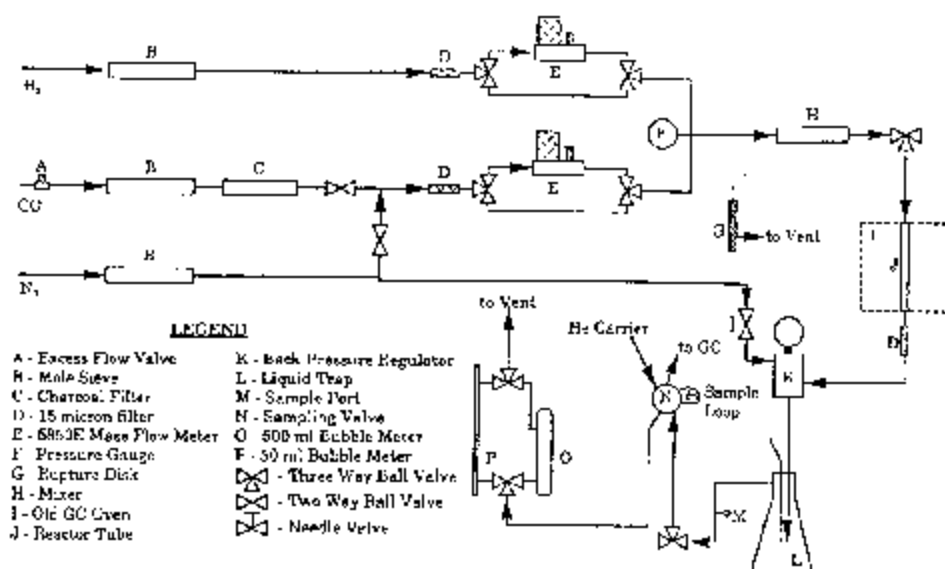


Figure 5. Schematic Diagram of Bench Top Reactor System #1.

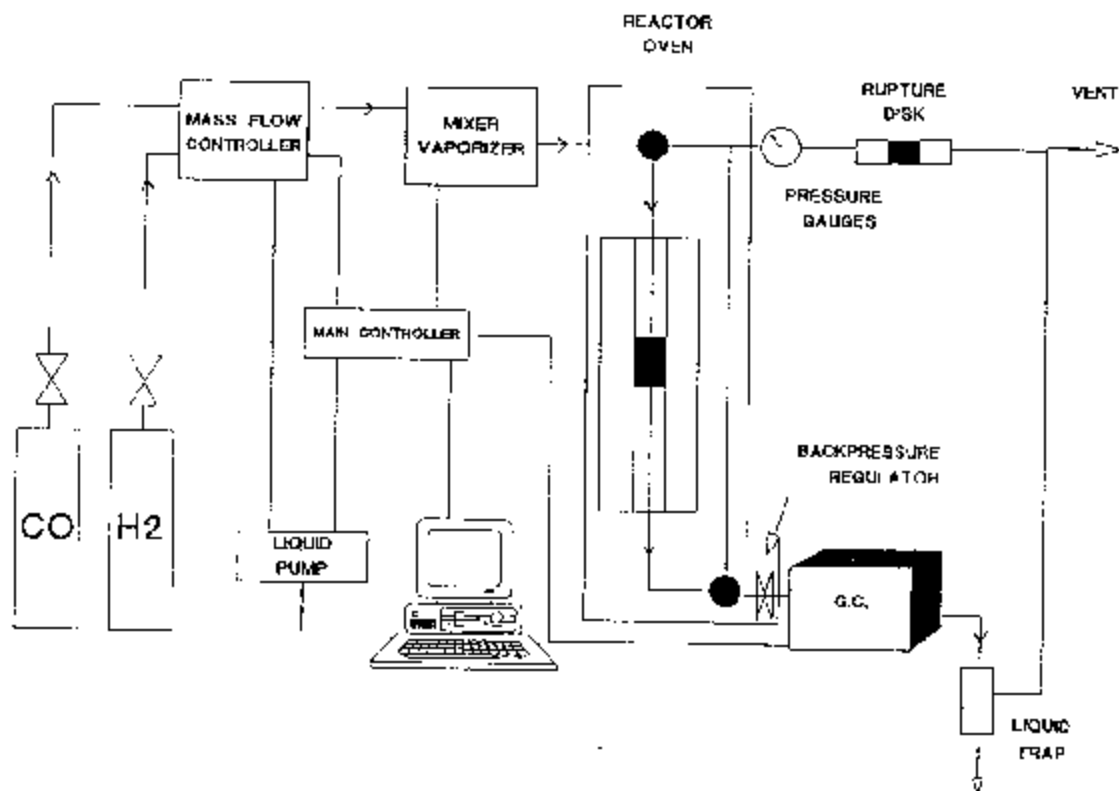


Figure 6. Schematic Diagram of AE MSBTR 900 (Formerly CDS 900) Reactor System

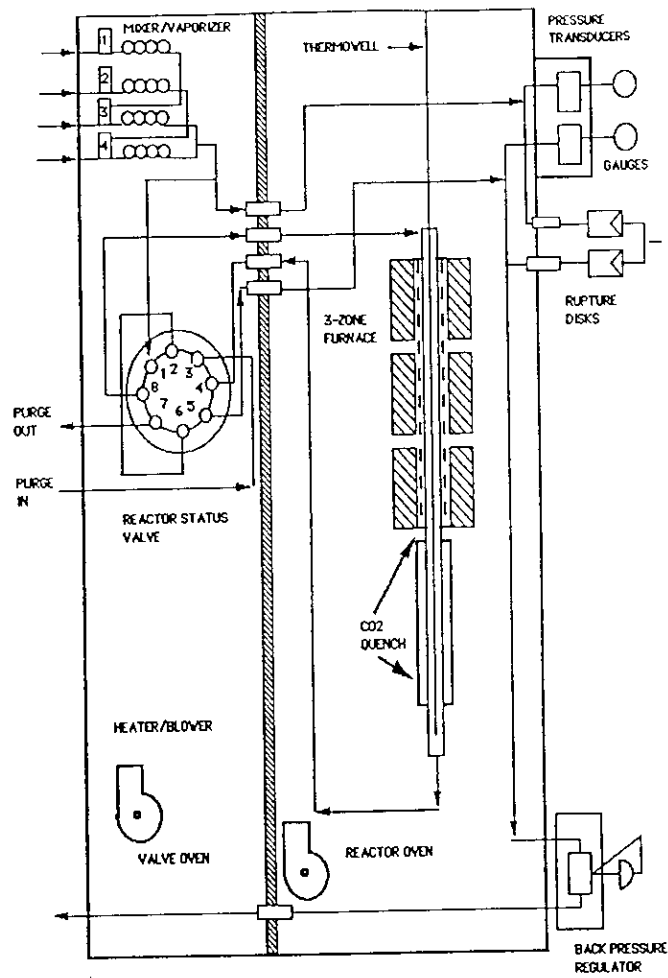


Figure 7. Reactor, Reactor Oven and Switching Valve Oven for AE MSBTR 900

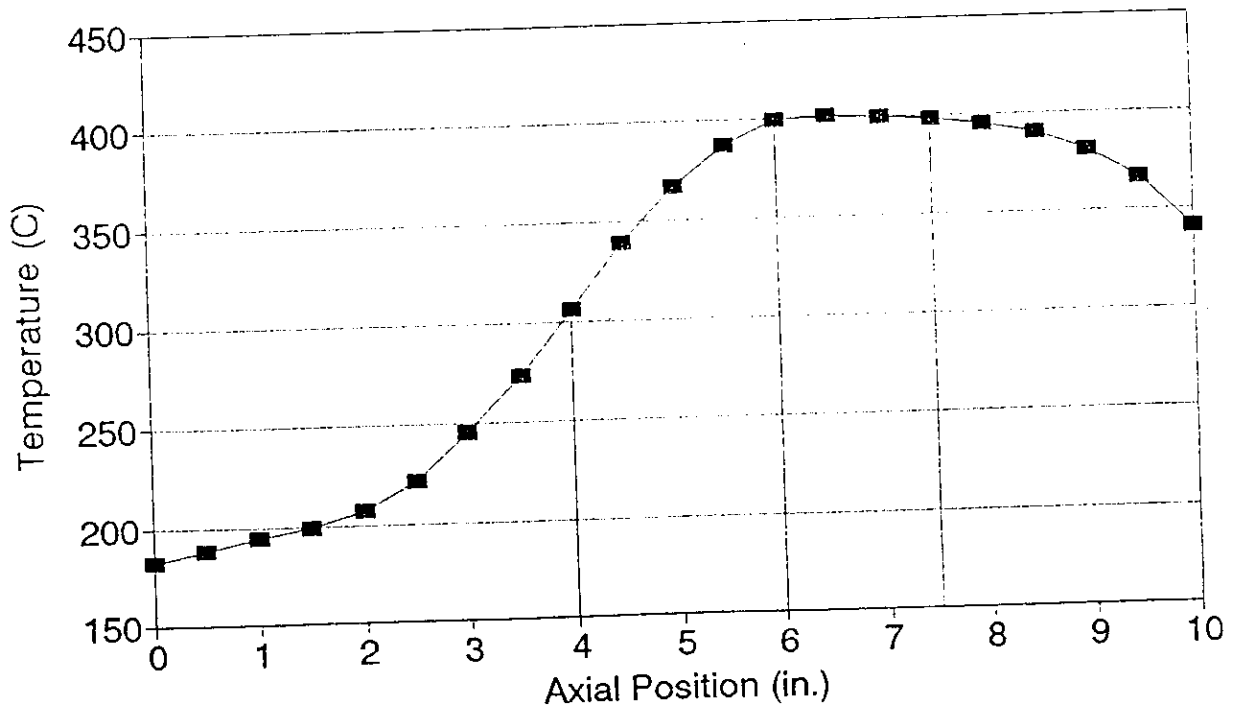


Figure 8. Typical Temperature Profile in the Reactor

Simulation of Temperature Profiles for CDS reactor system
(N₂ Flow, Heating Jacket Temp = 410 C, Oven temp = 160 C)

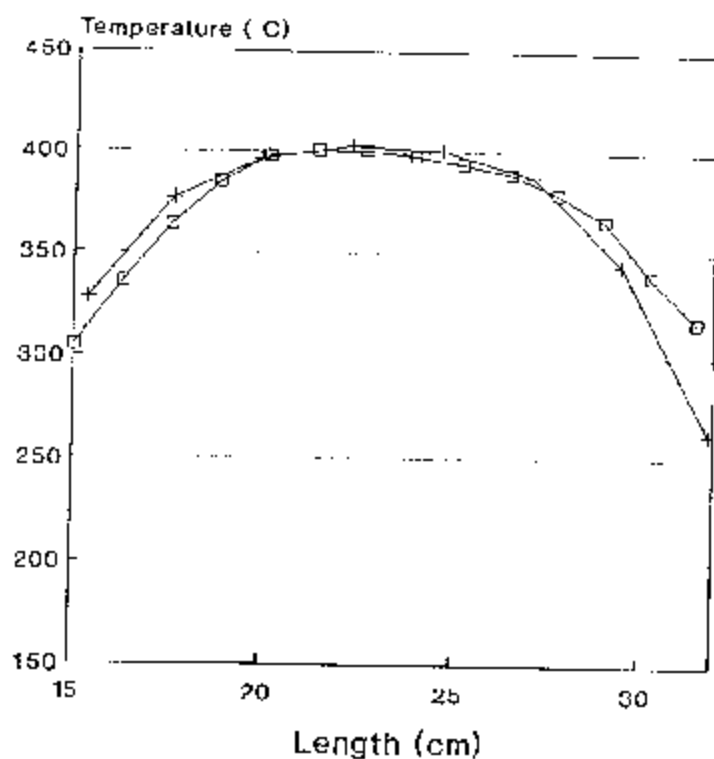


Figure 9. Actual and Calculated (Simulated) Reactor Profile for AE MSBTR 900

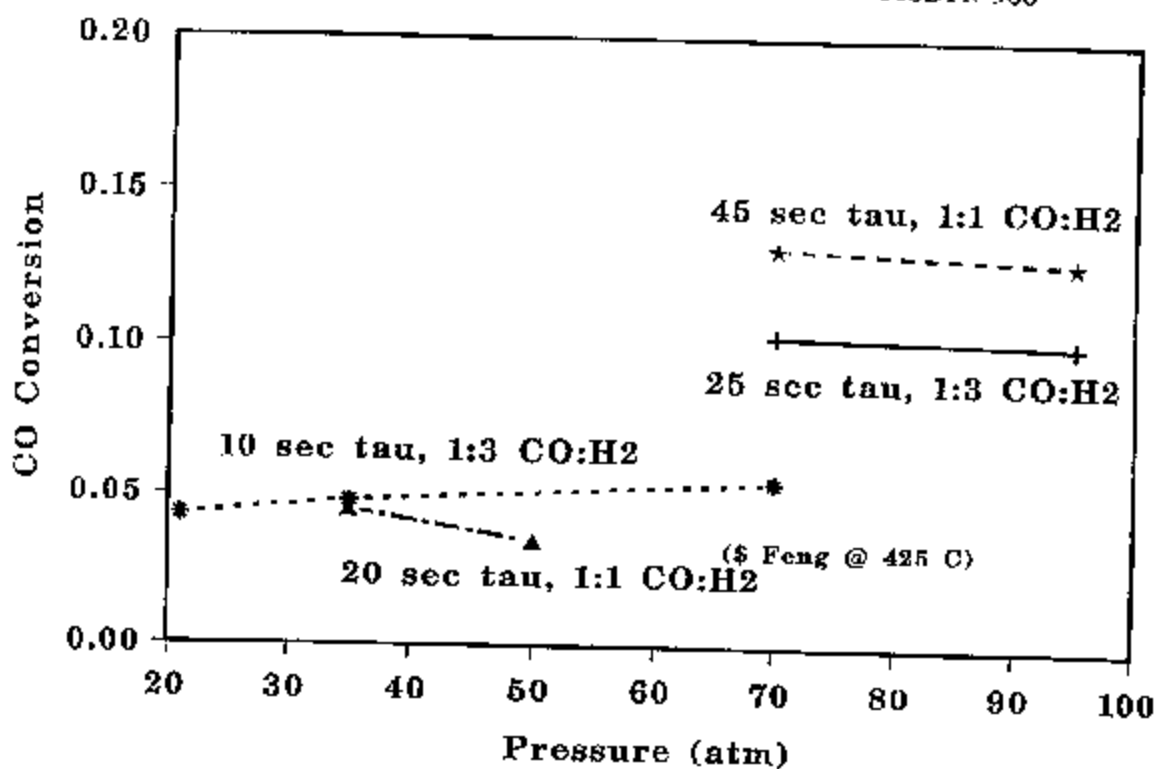


Figure 10. Activities and Effect of Pressure on Activity for Catalysts #1 and #2. (Cat. 2 is indicated by the (\$ Feng @ 425 °C)).

CO:H₂ Ratio at 95 atm & 400 C

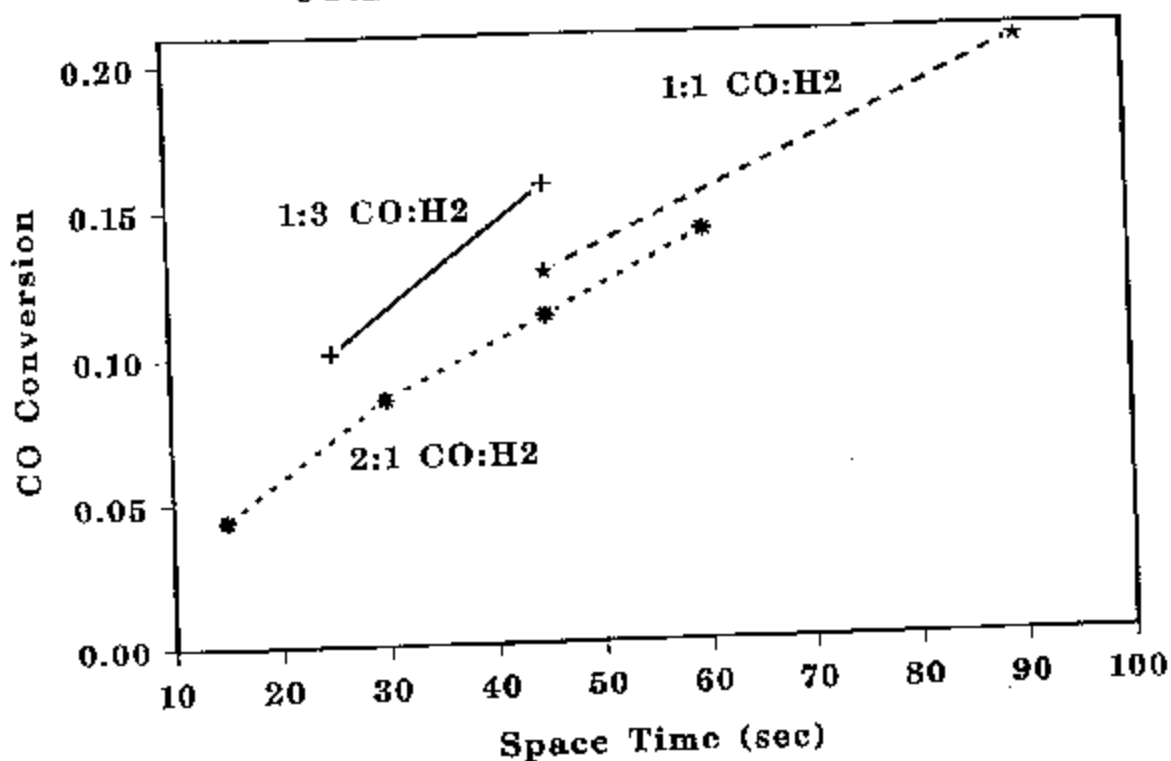


Figure 11. Activity as a Function of Space Time and Feed Ratios for Cat. #1.

CO/H₂ 1:1, 50 atm, 425 C

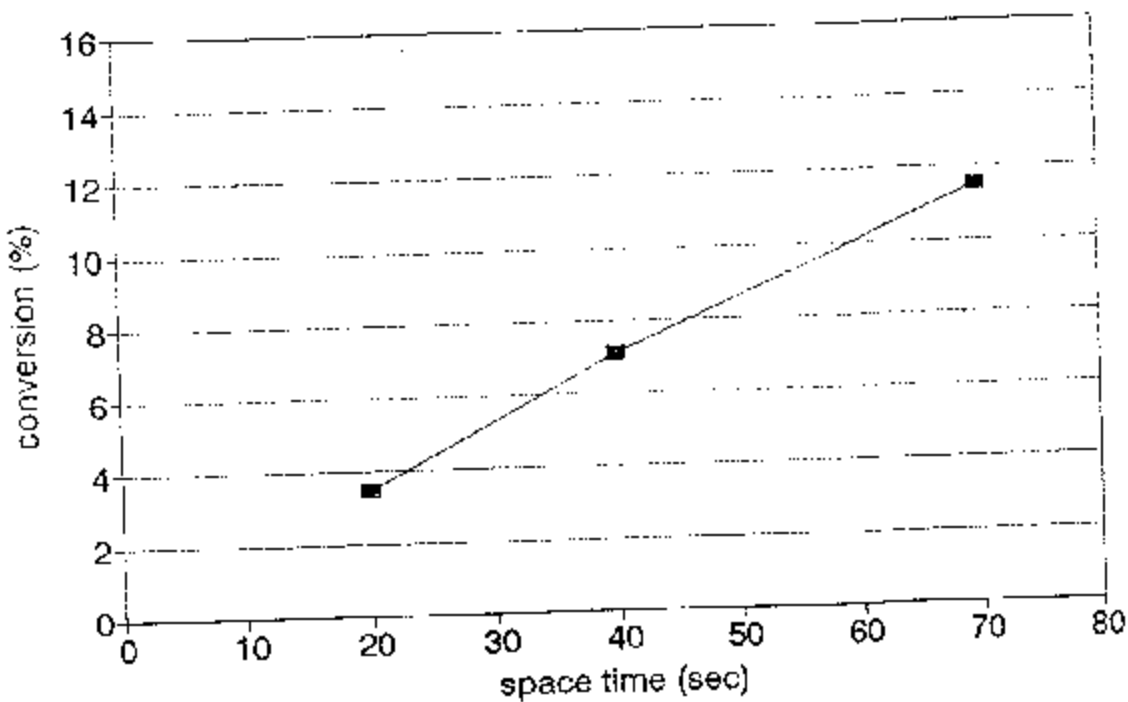


Figure 12. Activity of Catalyst #2.

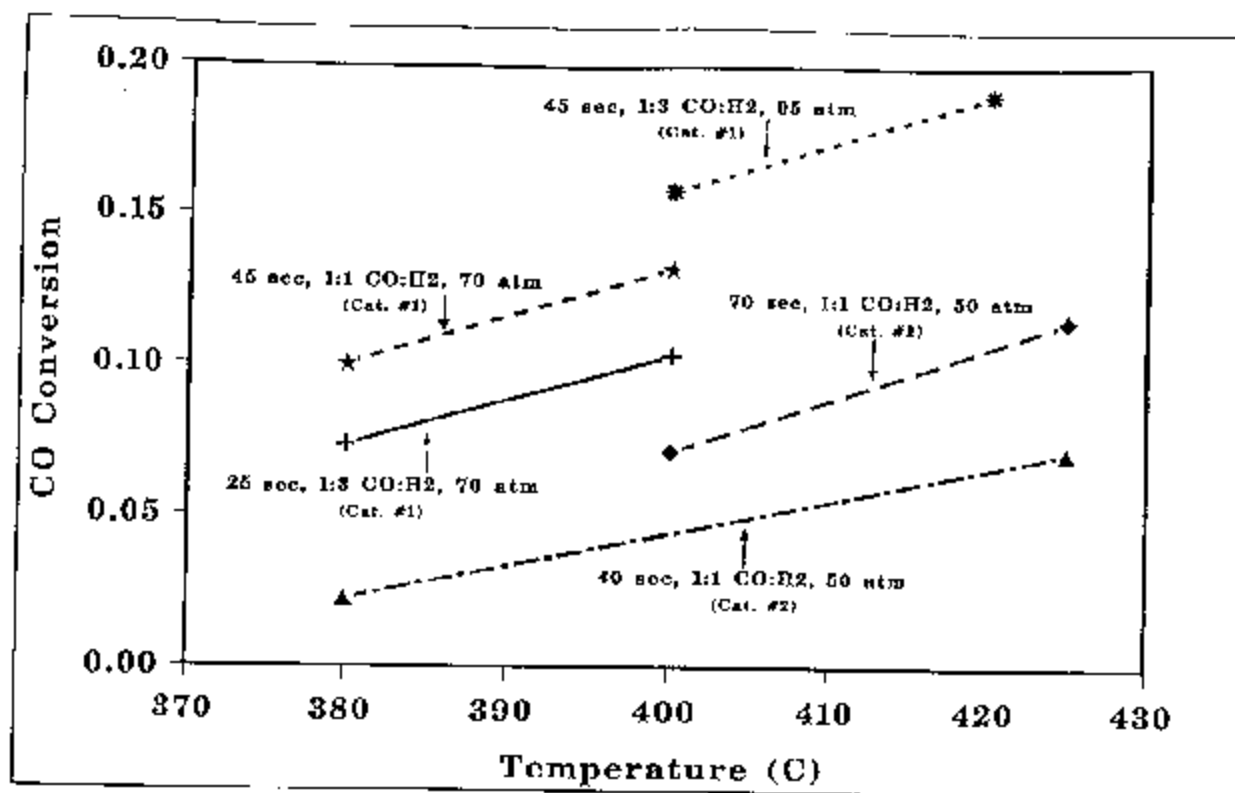


Figure 13. Comparison of Activities of Catalyst 1 and 2. Trends with respect to temperature are the same.

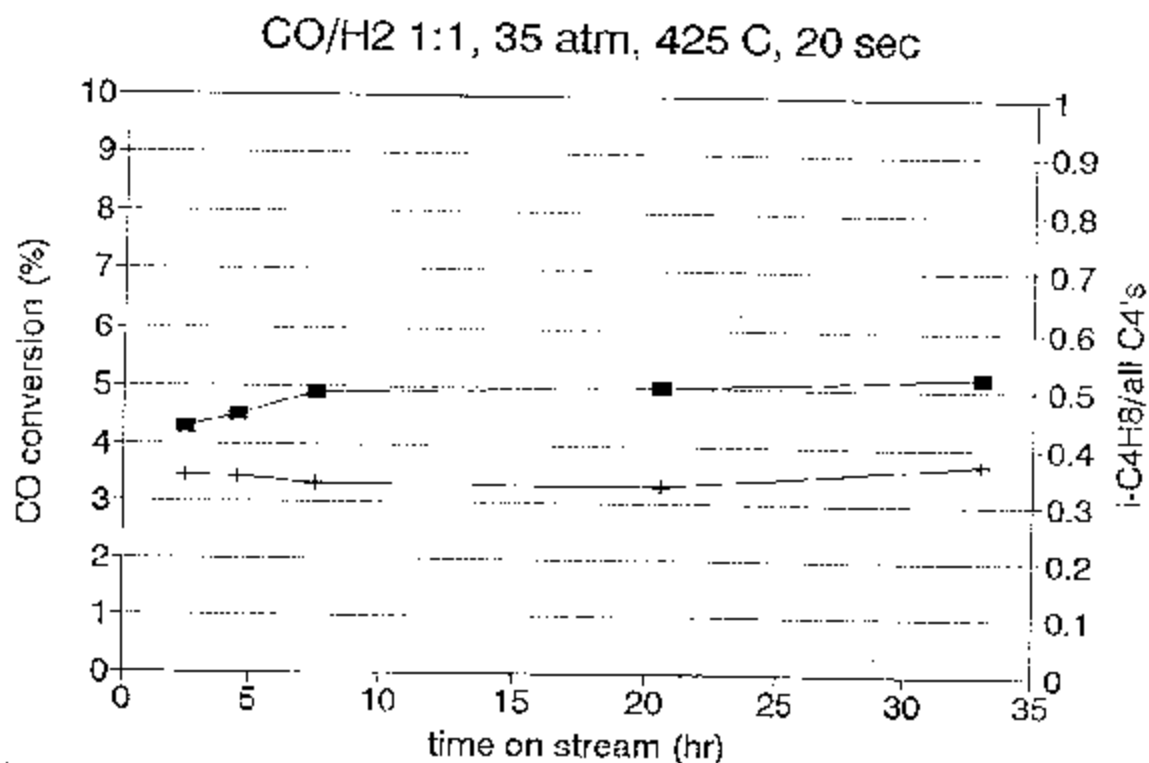
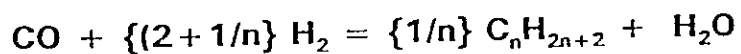
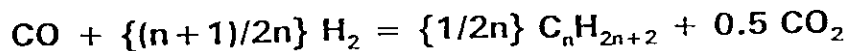


Figure 14. Selectivity and Conversions for Cat. 2 with Time on Stream.

ALKANES



OLEFINS

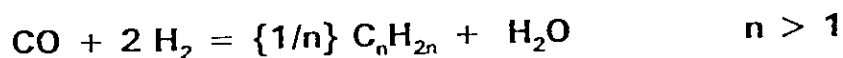
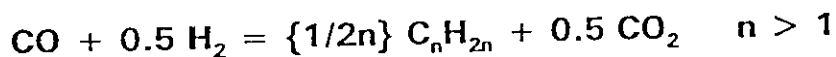


Figure 15. Potential Reaction Stoichiometry For Formation of Hydrocarbons.

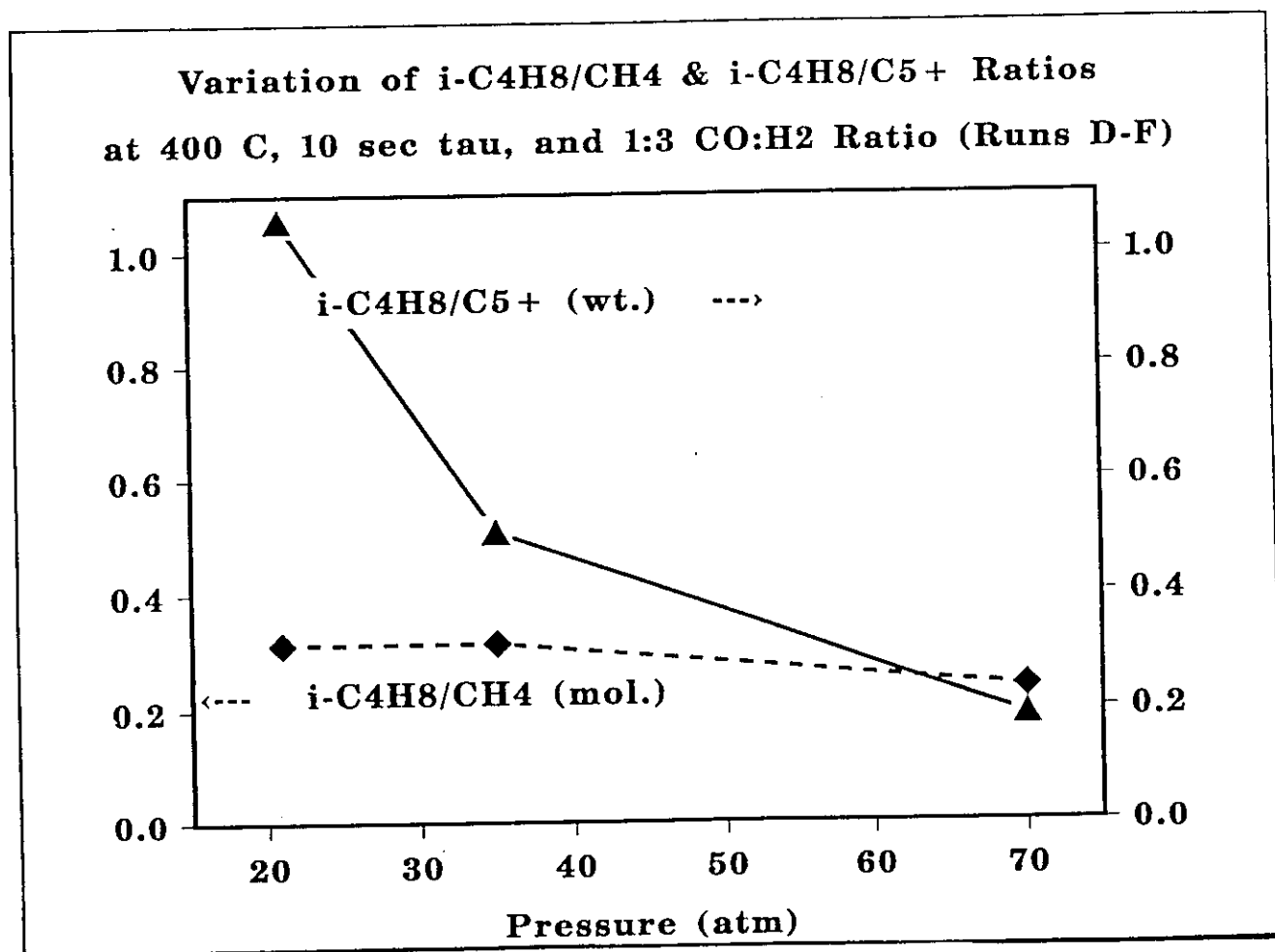


Figure 16. Effect of Pressure on Selectivities for Catalyst #1.

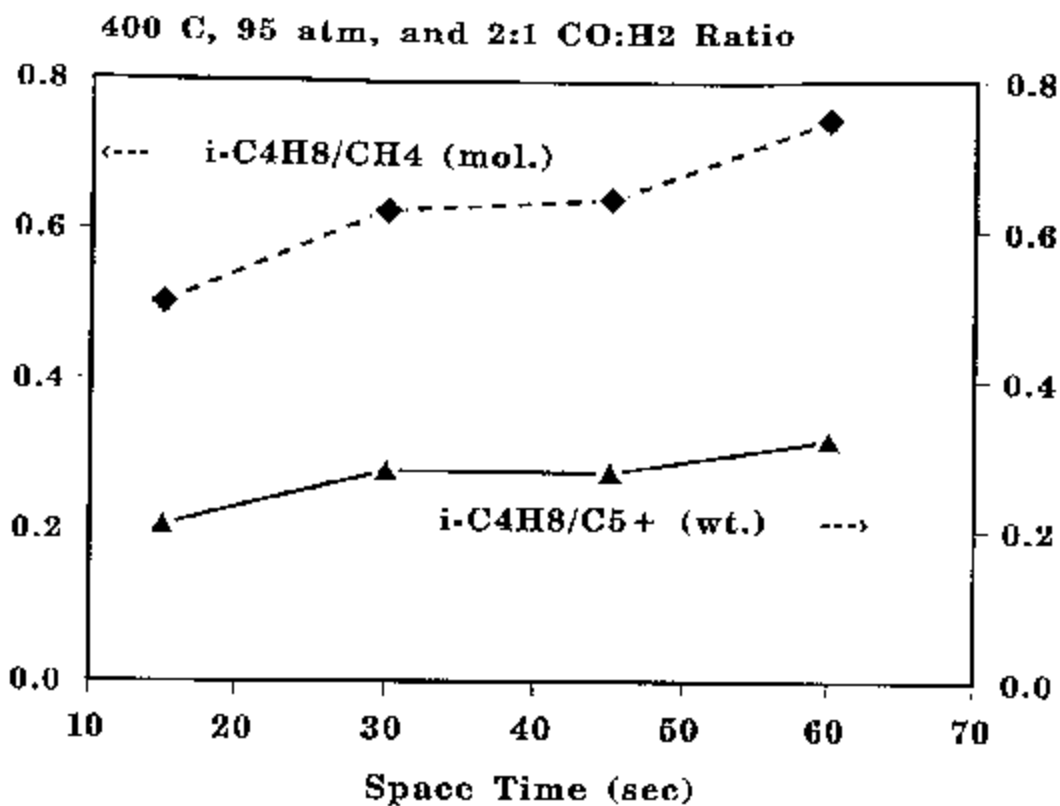


Figure 17. Selectivities For Catalyst #1.

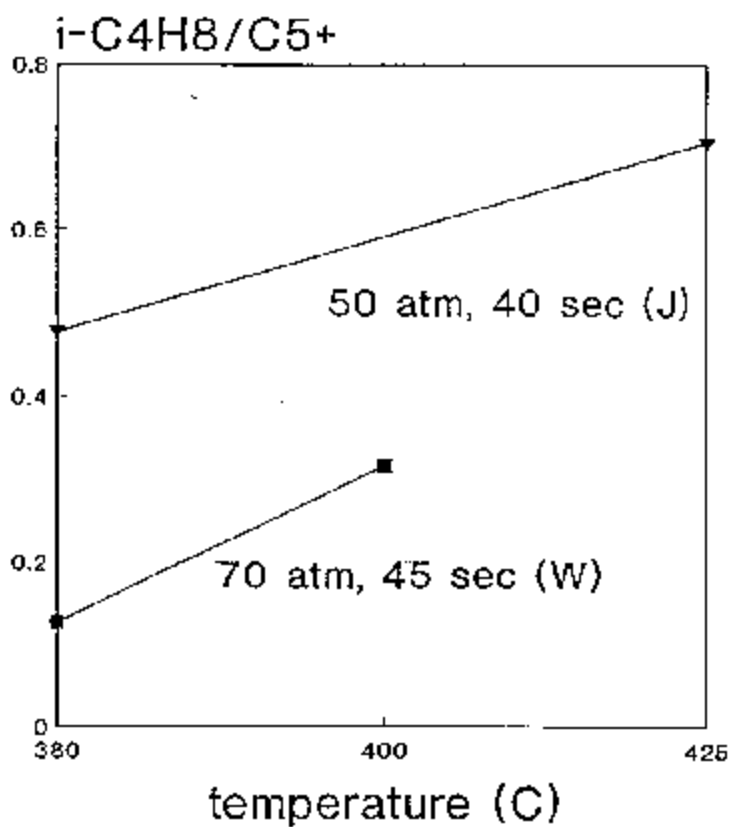


Figure 18. Weight Ratio of Isobutylene to C₅⁺ Increases with Temperature For Cat. 1 and 2.

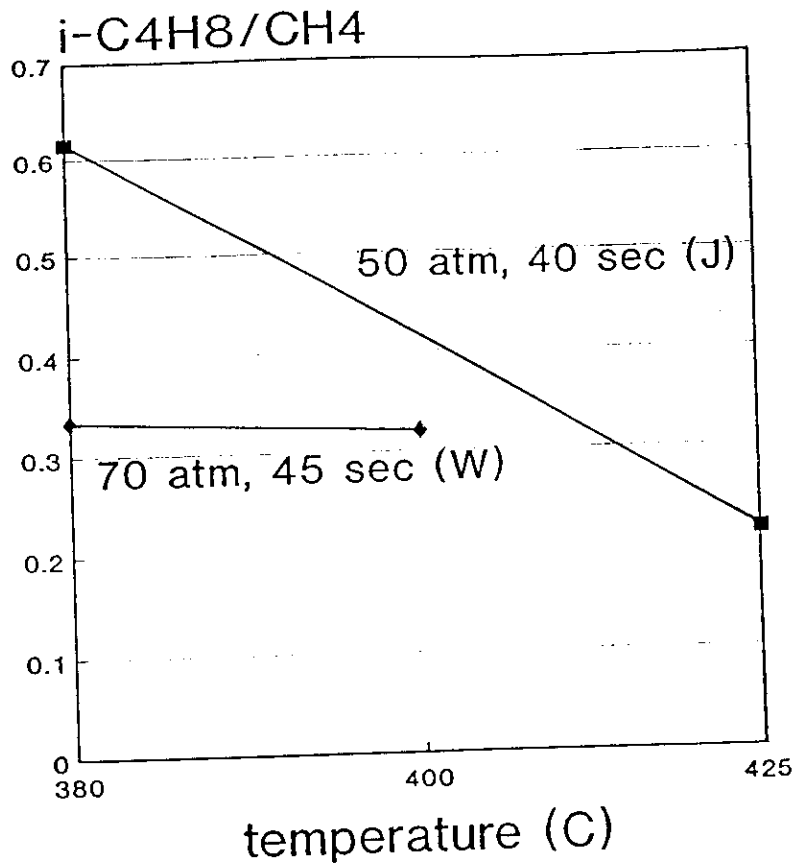


Figure 19. Weight Ratio of Isobutylene to Methane for Cat. 2 (J) and Cat. 1 (W).

Conversion @70 atm & 1:3 CO:H₂ Feed

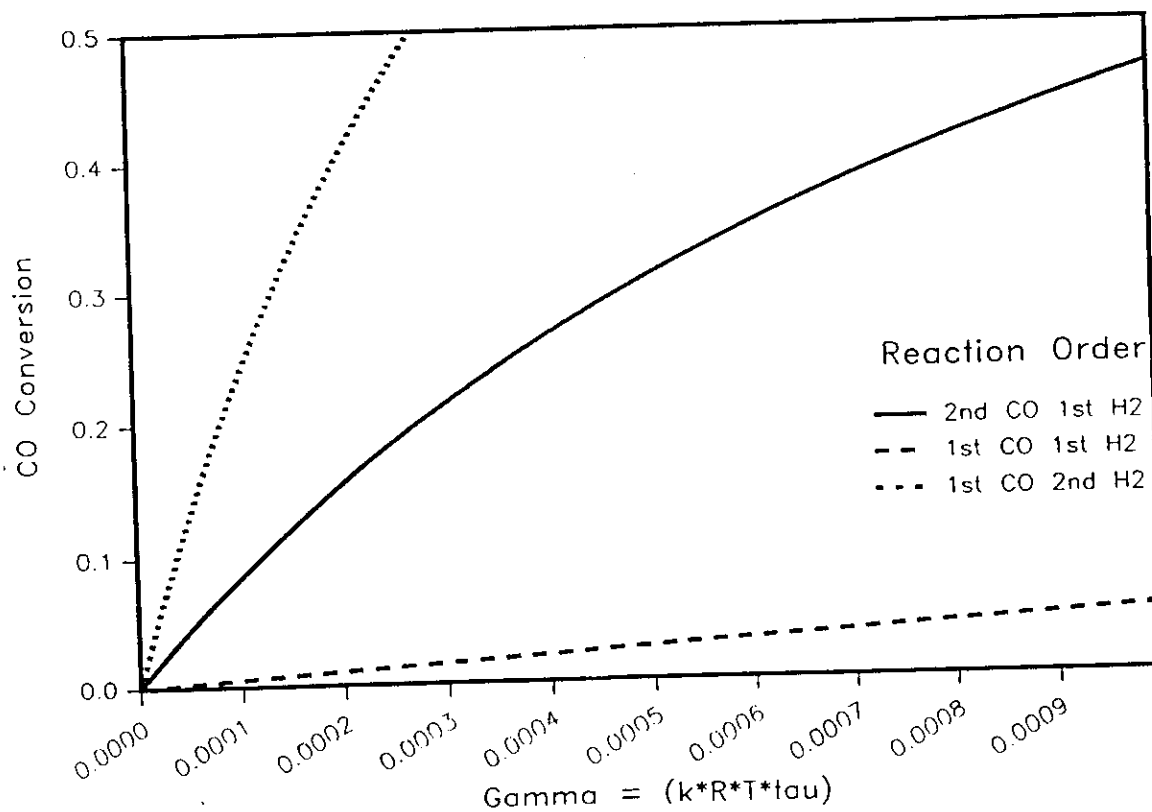


Figure 20. Calculated Conversions For Plug Flow Reactor With CO:H₂ Ratio of 1:3.

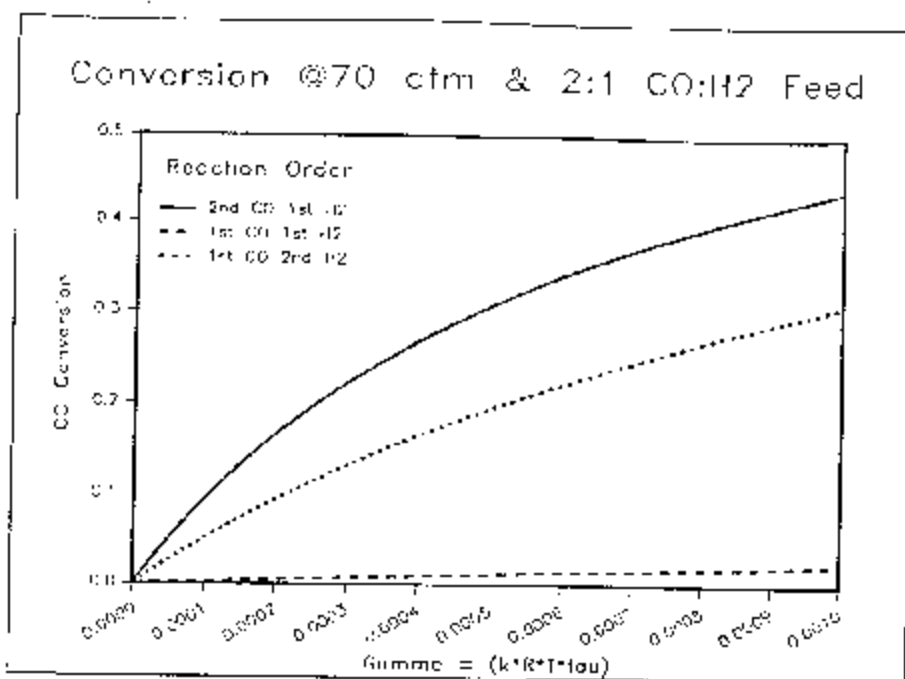


Figure 21. Calculated Conversions For Plug Flow Reactor With CO:H₂ Ratio of 2:1.

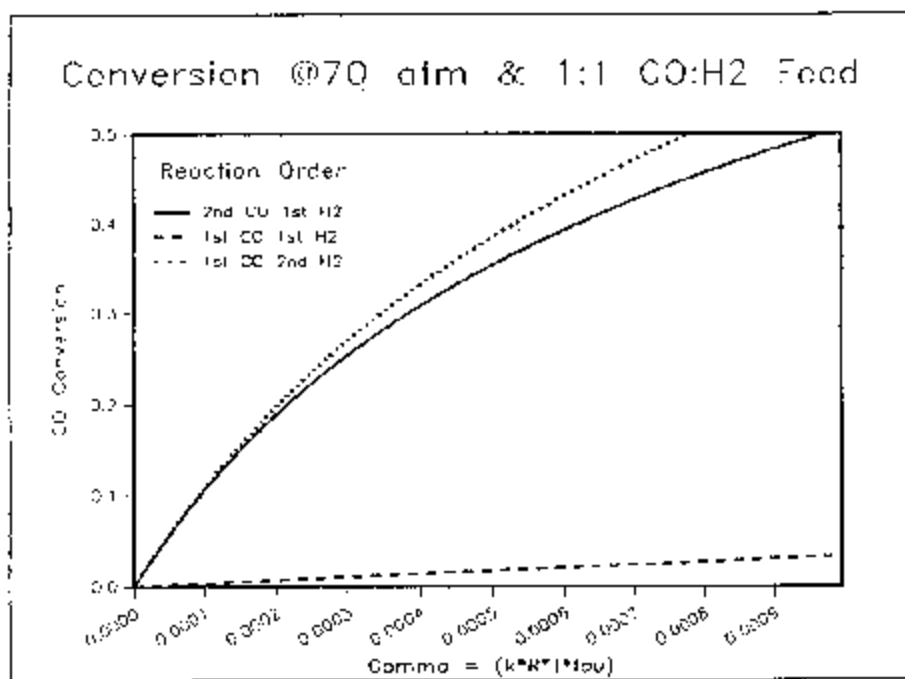


Figure 22. Calculated Conversions For Plug Flow Reactor With CO:H₂ Ratio of 1:1.

TRICKLE BED REACTOR MODEL

A two-dimensional three-phase isothermal trickle bed reactor with axial mixing, flux boundary conditions and a nonlinear reaction



The gas phase

$$\frac{\partial Y}{\partial Z} + F_L \cdot W^\circ \cdot \left(\frac{K}{H} \cdot Y - X \right) + (1-f) \cdot F_{gs} \cdot W^\circ \cdot \left(\frac{K}{H} \cdot Y - X_s \right) \Big|_{U=1} = 0$$

The liquid phase

$$\frac{\partial^2 X}{\partial Z^2} - P_{el} \cdot \frac{\partial X}{\partial Z} + P_{el} \cdot F_L \cdot \left(\frac{K}{H} \cdot Y - X \right) - f \cdot P_{el} \cdot F_{ls} \cdot (X - X_s) \Big|_{U=1} = 0$$

The solid phase

$$U \cdot \frac{\partial^2 X_s}{\partial U^2} + \frac{3}{2} \cdot \frac{\partial X_s}{\partial U} = \frac{1}{4} \cdot \mathcal{R}$$

with

$$\mathcal{R}_i = D_{f_i} \cdot \prod_i X_{s,i}^{a_i} - D_{b_i} \cdot \prod_i X_{s,i}^{b_i}$$

Where

X and Y are dimensionless concentration vectors.

With boundary condition

$$Y_i \Big|_{Z=0^+} = Y_i \Big|_{Z=0^-}$$

$$X_i \Big|_{Z=0^+} = X_i \Big|_{Z=0^-} - \frac{1}{P_{el}} \cdot \frac{\partial X_i}{\partial Z}$$

$$\frac{\partial X_i}{\partial Z} \Big|_{Z=1} = 0$$

$$\frac{\partial X_{s,i}}{\partial U} \Big|_{U=0} = \text{finite}$$

$$\frac{\partial X_{s,i}}{\partial U} \Big|_{U=1} = \frac{1}{2} \cdot f \cdot Sh_{l,i} \cdot (X_i - X_{s,i}) \Big|_{U=1} + \frac{1}{2} \cdot (1-f) \cdot Sh_{g,i} \cdot \left(\frac{K}{H_i} \cdot Y_i - X_{s,i} \right) \Big|_{U=1}$$

Figure 23. Trickle Bed Reactor Model In Dimensionless Variables.

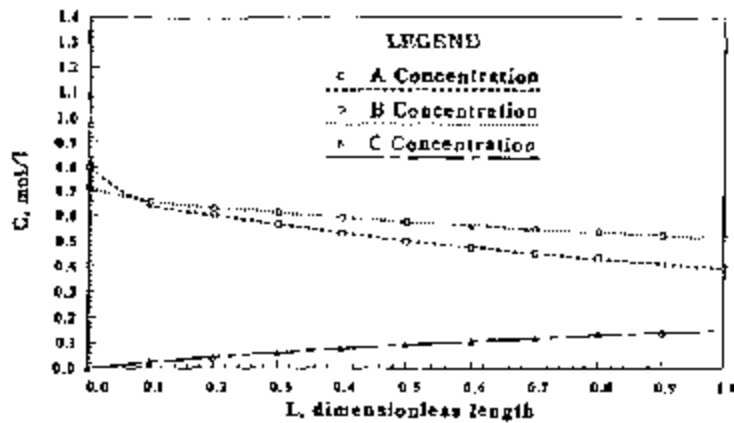


Figure 24. Calculated Gas Phase Profile For Model Presented in Figure 23.

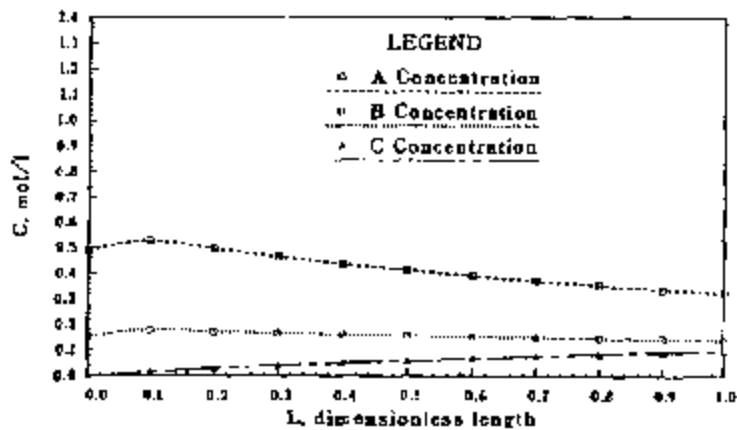


Figure 25. Calculated Liquid Phase Profile For Model Presented in Figure 23.

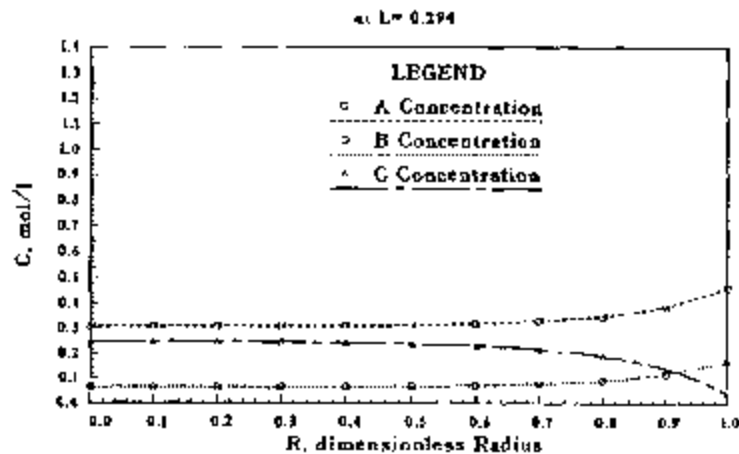


Figure 26. Calculated Solid Phase Profile For Model Presented in Figure 23 and Resistance to Pore Diffusion.